Check for updates

Received: 1 February 2025 | Revised: 25 February 2025 | Accepted: 19 March 2025

DOI: 10.1002/pen.27210

RESEARCH ARTICLE

POLYMER ENGINEERING AND SCIENCE WILEY

Thermal aging behavior and lifetime prediction of industrial elastomeric compounds based on styrene–butadiene rubber

Masoud Tayefi[1,2] | **Mostafa Eesaee**[1,2] | **Meysam Hassanipour**[3] | **Said Elkoun**[4] | **Eric David**[5] | **Phuong Nguyen-Tri**[1,2]

[1]Department of Chemistry, Biochemistry and Physics, Université du Québec à Trois-Rivières (UQTR), Trois-Rivières, Quebec, Canada

[2]Laboratory of Advanced Materials for Energy and Environment, Université du Québec à Trois-Rivières (UQTR), Trois-Rivières, Quebec, Canada

[3]Hydro-Québec Research Center, Varennes, Québec, Canada

[4]Center for Innovation in Technological Eco-Design (CITE), University of Sherbrooke, Sherbrooke, Quebec, Canada

[5]Mechanical Engineering Department, École de Technologie Supérieure (ETS), Montréal, Quebec, Canada

Correspondence
Phuong Nguyen-Tri, Department of Chemistry, Biochemistry and Physics, Université du Québec à Trois-Rivières (UQTR), 3351 Boulevard des Forges, Trois-Rivières, QC G8Z 4M3, Canada.
Email: phuong.nguyen-tri@uqtr.ca

Funding information
Natural Sciences and Engineering Research Council of Canada

Abstract

This work describes the thermal aging behavior of three industrial elastomeric compounds based on styrene–butadiene rubber (SBR) reinforced with carbon black. Samples were exposed to thermo-oxidative aging at temperatures ranging from 70 to 120°C for durations between 14 and 365 days. The tensile and hardness tests were performed on the samples to determine changes in their mechanical properties. Upon aging, hardness and 100% modulus increased, while elongation at break decreased for all three samples. The results showed a significant decrease in elongation at break and an increase in hardness and modulus with prolonged aging time and higher temperatures. For instance, the elongation at break of the three types of samples decreased by approximately 50% in less than 90 days at 70°C, whereas at 120°C, this same level of degradation occurred in less than 2 days. These significant changes were correlated with increased brittleness and reduced flexibility of SBR composites. Swelling tests confirmed an increase in crosslink density due to aging. Laser scanning confocal microscopy revealed surface roughness and defects, attributed to oxidation, crosslinking, and the evaporation of low molecular weight components. Lifetime prediction methods, including the Arrhenius equation and time–temperature superposition (TTS), were applied to estimate the service life of the materials. The Ahagon plot was utilized to understand the aging mechanisms, revealing a transition from crosslinking-dominated degradation to chain scission processes at higher temperatures and longer aging times.

Highlights

- Thermal aging makes SBR compounds more brittle and less flexible over time.
- The hardness and stiffness of SBR compounds increase with aging temperature and time.
- Aging increases crosslink density, confirmed by swelling tests.

This is an open access article under the terms of the Creative Commons Attribution-NonCommercial-NoDerivs License, which permits use and distribution in any medium, provided the original work is properly cited, the use is non-commercial and no modifications or adaptations are made.
© 2025 The Author(s). *Polymer Engineering & Science* published by Wiley Periodicals LLC on behalf of Society of Plastics Engineers.

- Increased surface roughness and defects due to oxidation and crosslinking.
- The aging mechanism shifts from crosslinking to chain scission at higher temperatures.

KEYWORDS

lifetime prediction, mechanical property degradation, styrene–butadiene rubber, thermal aging, time–temperature superposition

1 | INTRODUCTION

Elastomers are indispensable in numerous industries such as automotive, aerospace, and construction due to their exceptional mechanical properties and their ability to function for a wide range of temperatures, especially at lower temperatures. To ensure that products made from elastomers perform reliably and endure over time, it is crucial to study how these materials handle dynamic and static stresses and withstand harsh environmental conditions. For example, exposure to high temperatures can accelerate the aging process of elastomers, causing significant changes in their mechanical, physical, and chemical properties.[1]

Styrene–butadiene rubber (SBR), created through the copolymerization of styrene and butadiene, contains unsaturated bonds due to the butadiene component. This necessitates the use of additives to protect it against oxygen, ozone, and UV light. SBR is primarily used in the tire industry, where it is blended with natural rubber (NR) and butadiene rubber (BR). Other applications include molded rubber parts, conveyor belts, and insulators.[2]

Several factors can contribute to the degradation of materials, including the substances they come into contact with, environmental conditions, and operating temperatures. Due to the significant impact of these factors, many studies have been dedicated to understanding how they influence material performance and longevity.[3–7] The degradation of elastomers is also a critical issue as it leads to the deterioration of their essential properties. This degradation process can be used to predict the materials' lifespan. Therefore, understanding the thermal aging behavior of elastomeric compounds is essential for predicting their service life and ensuring the reliability of products that incorporate these materials.[1]

As a consequence, during the past 2 years, several works have been done to study and improve the aging properties of the different elastomers.[8–12] Some studies have explored the effects of thermo-oxidative aging on the mechanical and chemical properties of SBR rubber,[13–15] revulcanized SBR,[16] and its thermal properties.[17] Additionally, the aging mechanism of SBR has been investigated using in situ thermal aging with 2D-FTIR equipment.[15,18] The comparison of SBR and nitrile rubber (NBR) composites showed that NBR demonstrated superior thermal resistance compared to SBR in terms of lifetime prediction.[19,20] For SBR and NBR rubber compounds, it was reported that gum vulcanizates have less change in 300% modulus than loaded samples upon aging, and the change intensified as carbon black (CB) content increased. This was related to the possible CB acceleration role of oxygen uptake in sulfur-cured rubber that caused faster rubber degradation and reduced stability.[20] However, other works reported that the carbon black did not affect the thermal aging process of NR[21] and polychloroprene rubber[22] compounds as the mechanical properties are directly influenced by the matrix network as it undergoes aging.[22] On the contrary, the increase in accelerator level was seen to have a positive effect on maintaining mechanical properties. It was related to the increase in disulfide and monosulfide content upon accelerated crosslinking that can enhance the thermal resistance of the rubber.[21]

In a recent study, the variation of carbon black (CB) levels effect on the properties of polychloroprene rubber, specifically through oxidative aging at 80°C in the air with CB concentrations ranging from 10 to 45 parts per hundred rubber (phr) was studied. Findings showed that the crosslinking behavior remained stable for different filler levels, and the mechanical properties are directly influenced by the matrix network as it undergoes aging.[22] Verifying the durability of these materials for specific applications is essential, especially since end-users often do not have access to the exact formulations of rubber compounds provided by suppliers.[1] For instance, there are some articles on the prediction of the lifetime of commercial rubbers, such as O-ring seals,[23–28] rubber insulators of cables used in nuclear power plants[29–31] and polymeric binders in solid propellants.[32–36] Due to this importance, the elastomer service life of elastomeric materials has been studied in our previous articles.[1,37,38]

In our previous article, the effect of additives on the aging behavior of different elastomers as well as the methodologies to predict the lifetime of elastomers were reviewed.[1,37] The study aims to investigate the thermal aging behavior of three industrial elastomeric compounds. Characterization tests have shown that

15482634, 0, Downloaded from https://4spepublications.onlinelibrary.wiley.com/doi/10.1002/pen.27210 by Ecole De Technologie Superieur, Wiley Online Library on [23/04/2025]. See the Terms and Conditions (https://onlinelibrary.wiley.com/terms-and-conditions) on Wiley Online Library for rules of use; OA articles are governed by the applicable Creative Commons License

TABLE 1 The compositions of materials.

Composition	E	A	P
Organic part (%)	52.1 ± 0.2	51.1 ± 0.2	54.3 ± 0.2
Extractable low molecule weight materials (%)[a]	9.1 ± 0.2	6.9 ± 0.2	5 ± 0.2
Carbon black (CB) (%)	31.1 ± 0.2	36.8 ± 0.2	36.1 ± 0.2
Inorganic filler (%)	7.7 ± 0.2	5.2 ± 0.2	4.6 ± 0.2

[a]Using TGA (confirmed by acetone extraction).

these compounds are based on SBR containing carbon black. Our goal is to analyze the changes in mechanical properties, physical characteristics, and microstructural properties of these compounds due to thermal exposure. Finally, two methods, the Arrhenius method and time–temperature superposition (TTS), were utilized to predict the material's lifetime. The findings will improve our understanding of the thermal aging mechanisms in elastomers and assist in the design and selection of materials for various industrial applications.

2 | EXPERIMENTAL

2.1 | Materials

Three types of industrial samples based on elastomeric compounds were used in this study. These materials were industrial elastomeric parts functioning in the electrical networks. The difference between them is their application. As the materials were required to serve in their application for the intended period, these materials became the research subject of this paper. Upon the preliminary part of the project, an attempt was made to characterize them using reverse engineering. The codes and compositions of materials are tabulated in Table 1. The results of Fourier-transform infrared spectroscopy (FTIR) demonstrated that they were based on SBR as the polymer matrix. To find out the percentages of additives, thermogravimetric analysis (TGA) was used.

2.2 | Thermal aging procedure

The samples were subjected to controlled thermal aging in a high-temperature oven. Various aging temperatures, ranging from 70 to 120°C, and durations were chosen to simulate accelerated aging conditions. The accelerated thermal aging process was performed following the ISO 11346 standard. The samples were periodically removed from the oven at predetermined intervals, cooled to room temperature, and then subjected to mechanical and microstructural analysis. At each interval, six samples were removed from the oven and tested, and the average of six repetitions was considered as the result. The methodology of accelerated thermal aging is depicted in Figure 1. To compare the change of the properties during the accelerated thermal aging time, the normalized property can be used to have a much better understanding of the change. The normalized property is defined as follows:

$$\text{Normalized property} = \frac{P_t}{P_0} \times 100 \quad (1)$$

In which, P_t is the property at the given aging time and P_0 is the property for the unaged sample.

2.3 | Microstructural analysis

Microstructural changes in the compounds were examined using a high-resolution laser scanning confocal microscope (LCSM) (Keyence VK-X1000, Japan). The microscope employs a 404 nm violet laser and has a Z-axis resolution of 5 nm. The images were captured at various magnifications to analyze the formation of surface irregularities including roughness, microcracks, voids, and surface defects.

2.4 | Mechanical analysis

To assess the tensile characteristics of the specimens, the Instron 4201 machine from Instron, USA, was employed, and the examination followed the guidelines outlined in the ASTM D 412 standard. Based on the standard, the rate of grip movement was 500 mm/min. The hardness of the vulcanizates was measured according to ASTM D2240 using a Shore A hardness tester (Bareiss, Germany) by layering four sheets together. The mechanical properties of the elastomeric compounds, including tensile strength, elongation at break, and hardness, were evaluated using standard testing procedures. The measurements were performed at regular intervals during the accelerated thermal aging process to monitor changes in mechanical properties.

15482634, 0, Downloaded from https://4spepublications.onlinelibrary.wiley.com/doi/10.1002/pen.27210 by Ecole De Technologie Superieur, Wiley Online Library on [23/04/2025]. See the Terms and Conditions (https://onlinelibrary.wiley.com/terms-and-conditions) on Wiley Online Library for rules of use; OA articles are governed by the applicable Creative Commons License

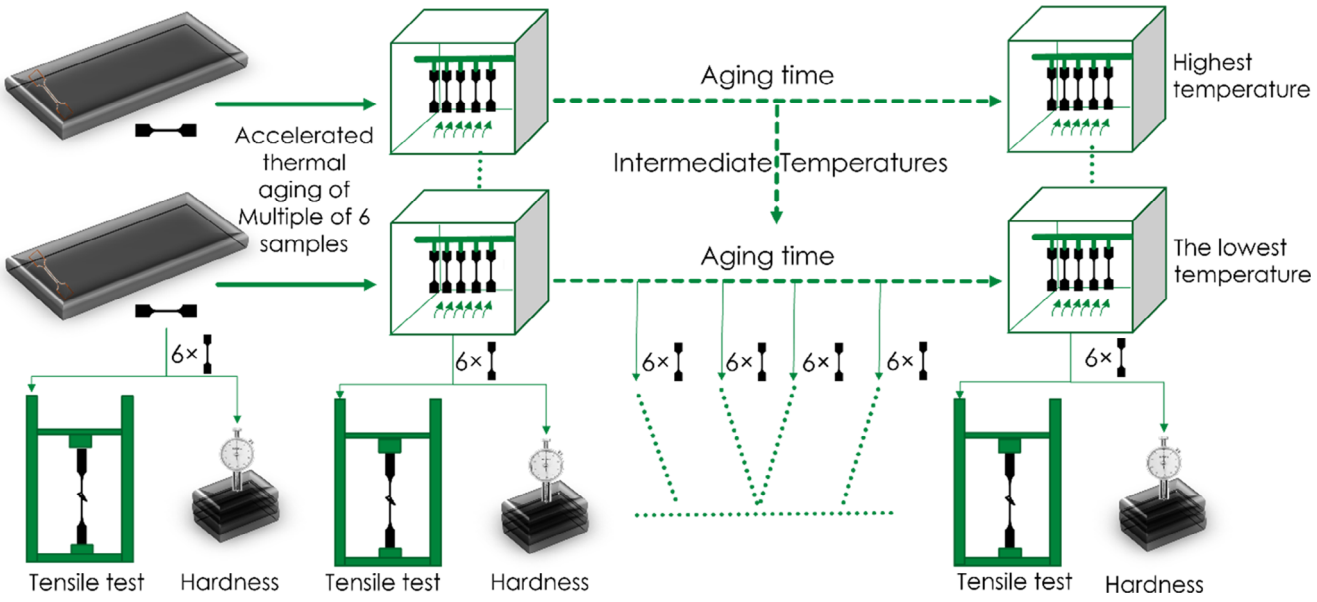

FIGURE 1 Methodology of accelerated thermal aging; The samples were subjected to controlled thermal aging at various temperatures, ranging from 70 to 120°C. Testing was conducted at regular intervals, with six samples evaluated at each time point.

2.5 | Thermogravimetric analysis

Thermogravimetric analysis (TGA) was performed on a PerkinElmer TGA 8000 (USA) under N_2 atmosphere from ambient temperature up to 750°C with a heating rate of 10°C/min.

2.6 | Swelling test

The swelling test is conducted on samples in line with ISO 1817 to evaluate the cross-link density of the samples. Toluene is used as the swelling solvent. Initially, the initial weight of the samples (w_i) is measured. Then the samples are immersed into toluene over 72 h at room temperature. After the swelling period, the samples are taken out and any excess solvent is removed using filter paper. The weight of the swollen samples (w_s) is then measured. Finally, the samples are dried by oven drying at 70°C for 2 h to achieve the dry weight (w_d). Once dried, the weight of the dried samples is recorded, and the rubber's volume fraction (v_r) is then calculated using the following equation:

$$v_r = \frac{1}{1+\frac{\rho_r}{\rho_t}\left(\frac{w_s-w_d}{w_d}\right)} \tag{2}$$

where ρ_r represents the density of the rubber, and ρ_t refers to the density of toluene. w_s is the weight of the swollen sample, while w_d is the weight of the dried rubber sample. Finally, the cross-link density of the rubber samples is determined using the Flory–Rehner equation:

$$\rho_c = -\frac{1}{2v_s} \times \frac{\ln(1-v_r)+v_r+\chi {v_r}^2}{{v_r}^{\frac{1}{3}}-0.5\,v_r} \tag{3}$$

where ρ_c represents the cross-link density of the rubber sample in mol/g, while v_r indicates the volume fraction of the rubber. v_s refers to the molar volume of the solvent, with a value of 106.36 cm^3/mol, and χ stands for the rubber–solvent interaction parameter for sulfur-cured SBR and toluene, which is calculated to be 0.42 on average within the cross-link density range under study.[39]

To calculate the swelling ratio, the following equation was used:

$$\text{Swelling}\,(\%) = \frac{(w_s-w_i)}{w_i} \times 100 \tag{4}$$

where the w_i and w_s are the weights of the initial and the swollen rubber, respectively.

2.7 | Lifetime prediction

To predict the service lifetime, the Arrhenius equation and TTS were used. The Arrhenius method for accelerated aging involves monitoring the property of an elastomer at various temperatures over time to determine its failure point—such as when it retains only 50% of its original properties. By plotting the logarithm of the

15482634, 0, Downloaded from https://4spepublications.onlinelibrary.wiley.com/doi/10.1002/pen.27210 by Ecole De Technologie Superieur, Wiley Online Library on [23/04/2025]. See the Terms and Conditions (https://onlinelibrary.wiley.com/terms-and-conditions) on Wiley Online Library for rules of use; OA articles are governed by the applicable Creative Commons License

property against the reciprocal of temperature, one can extrapolate and predict the elastomer's service life.[1] The Arrhenius equation used for this purpose is as follows[40]:

$$t = A \times e^{(-E_a/RT)} \quad (5)$$

where t represents the time to reach a 50% change of the property, A is the pre-exponential factor, E_a, R, and T represent the activation energy in kJ/mol, the universal gas constant 8.314 J/(mol K), and the absolute temperature in kelvin, respectively.

Another approach used in the study was the TTS, where data from each temperature level is shifted along the time (X) axis to align with the data at a reference temperature. This involves adjusting each curve so that the endpoint of one aligns with the starting point of the next temperature curve. Repeating this process for all temperature datasets generates the TTS curve.[1]

3 | RESULTS AND DISCUSSION

3.1 | Microstructural analysis

The results of microscopy images of unaged and highest time, 18 days, aged at 100°C and their corresponding 3d surface for sample E were shown in Figure 2. The microscopy of samples' surfaces before aging demonstrated that samples' surfaces were smooth and continuous As it is visible by zooming in the area under the test, this condition is much more visible. However, the microscopy of the samples' surfaces after aging of samples showed that the samples showed a rough surface after aging with some round roughness produced by the accelerated thermal aging. With zooming in closer to the samples' surface, these images also clarified the higher roughness as well as the less continuous surface. As can be seen, the surface of the SBR composites became much rougher upon aging. This was a consequence of losing the low molecular weight upon aging, as well as the formation of agglomerations of fillers.[41,42]

For comparing the data obtained from microscopy, the roughness information of the surface of unaged and highest time aged at 100°C for E, P, and A samples are tabulated in Table 2. The arithmetical mean height (S_a) measures how much each point on a surface deviates from the average surface height. This parameter is commonly used to assess surface roughness. Maximum height (S_z) represents the combined value of the highest peak and the deepest hole within a specified area. As it can be seen for each sample, the higher S_a and S_z were obtained after aging, which means the formation of peaks with higher intensity upon this treatment can be due to evaporation of waxes and degradation of the surface. As observed, the highest change in S_a occurred in the order of E, A, and P. This trend correlates with the amount of low molecular weight materials in the samples, which was higher in the same order (E, A, and P), as confirmed by the TGA results.

3.2 | Mechanical properties

The stress–strain curves of tensile tests of samples are shown in Figure 3A–F. To reduce the number of images, since for the other temperatures between 70 and 120°C a

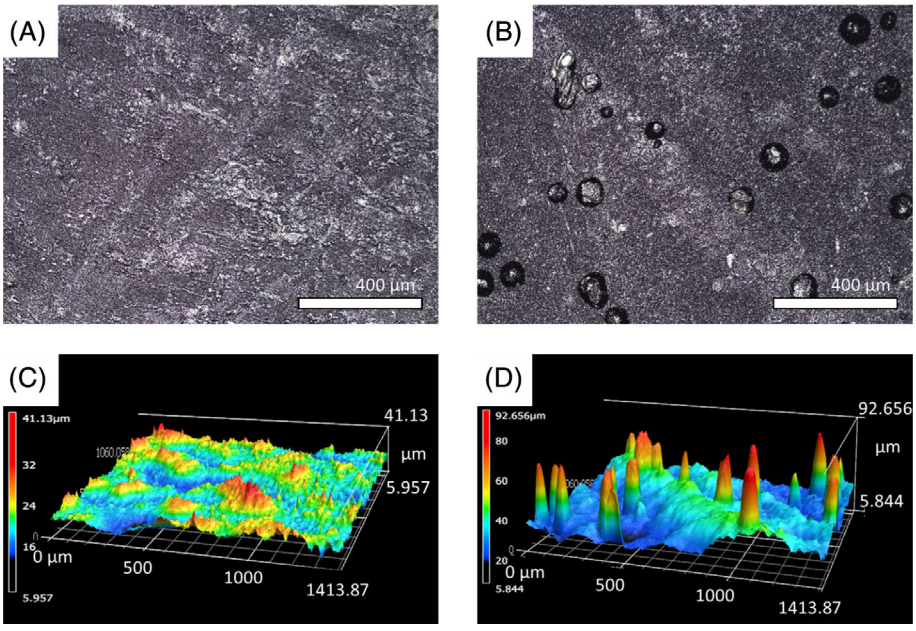

FIGURE 2 Microscopy images of (A) unaged and (B) 18 days aged at 100°C and their corresponding 3d surface (C) and (D) for sample E.

15482634, 0, Downloaded from https://4spepublications.onlinelibrary.wiley.com/doi/10.1002/pen.27210 by Ecole De Technologie Superieur, Wiley Online Library on [23/04/2025]. See the Terms and Conditions (https://onlinelibrary.wiley.com/terms-and-conditions) on Wiley Online Library for rules of use; OA articles are governed by the applicable Creative Commons License

TABLE 2 The roughness information of the surface of the samples.

Sample	S_a (μm)	S_z (μm)
E	2.61 ± 0.05	35.17 ± 0.50
E-aged 100°C-18 days	7.19 ± 0.20	86.81 ± 2.10
P	2.98 ± 0.05	40.51 ± 0.50
P-aged 100°C-18 days	3.49 ± 0.10	52.56 ± 1.24
A	1.89 ± 0.05	30.84 ± 0.50
A-aged 100°C-18 days	4.07 ± 0.20	89.89 ± 1.22

similar trend was observed, they were not shown here. The results revealed a significant decline in the elongation at the break of the elastomeric compounds with increasing aging time and temperature, indicating increased brittleness and reduced flexibility. Additionally, the rate of change in tensile properties was higher in the samples aged at higher temperatures, a trend consistent for all three elastomers. For example, to achieve the same change seen for 1 day at 120°C, the samples should be aged about 44 days at 70°C. This behavior was also reported for SBR,[14,43] silicone rubber,[44] polychloroprene rubbers (CR),[45] EPDM,[46] and HNBR.[47,48]

However, the change of tensile strength with aging time and temperature varied among the three types of compounds. For samples E and A, the effect of time of thermal aging on the tensile strength was not high at the given temperatures. Conversely, sample P exhibited a gradual decrease in tensile strength with aging time for all tested temperatures, indicating a loss of load-bearing capability. This was much more pronounced for higher temperatures as there was a sharp reduction in tensile stress for the P sample aged at 120°C (Figure 3A–F). These differences in the compounds' responses can be attributed to the type and percentage of protective ingredients used in their formulations and the variations in their initial crosslink density, which could cause a much ratio of chain scission/cross-linking. It has been reported that the higher amount of accelerators had a positive effect on the thermal aging of NR compounds by affecting the crosslink structure.[21] Furthermore, it has also been reported that the types and the percentage of three types of plasticizers, liquid butadiene (LB); paraffinic oil (PO); and polyethylene wax (PW) had a significant influence on the results of thermal aging of EPDM/CB compound.[49]

The normalized elongation at break and the 100% modulus versus aging time for different temperatures from 70 to 120°C were shown in Figure 4A–F. The elongation at break significantly reduced with increasing aging time. The reduction was more pronounced for samples aged at higher temperatures. In other words, the elongation at break reached a given normalized value sooner. The overall trend for elongation at break was the same for all three samples as it was governed mostly by the base of the polymeric matrix, which was the same for the three compounds. In other words, although there would be a loss of low molecular weight samples in the system, the elongation at break is significantly influenced by changes in the polymer matrix during aging; as crosslink density increases, SBR composites' extensibility decreases, and its rigidity increases. A nearly the same trend of the elongation at break reduction with thermo-oxidative aging was also seen for NBR,[50] EPDM,[41,42] SBR,[13,14] revulcanized SBR,[16] and fluorocarbon elastomer[51] which was related to the domination of the crosslinking reaction over the chain scission reaction upon thermo-oxidative aging.[42]

The overall trend for 100% modulus, stress at 100% elongation, upon aging time for the given temperatures was ascending as it was depicted in Figure 4A–F. Meanwhile, higher temperatures cause a much higher increase in the 100% modulus. It can be due to the increase in the crosslink density of polymer and the loss of low molecular weight samples in the system. It should be noted that for samples aged at elevated temperatures and/or for long durations, the 100% modulus could not be calculated because SBR composites became so brittle that they broke before reaching 100% strain. As a result, some data points for 100% modulus were not available in the figure. In addition, the change of 100% modulus was as E > A > P sample; this could be due to having the same order of low molecular weight material in the system and the types of protective additives used in their productions. An increase in modulus upon aging also was seen by other authors for butyl rubber.[3]

To ensure the minimum thickness required for the hardness test, four pieces of each sample were stacked for each sample, and five repetitions were carried out on the samples, with the median value selected as the result. To have a better comparison of the changes in the samples upon aging, the normalized hardness versus aging time for the different temperatures mentioned was represented in Figure 5. The hardening is more pronounced in the initial stages of aging, gradually slowing down as time progresses. A similar trend is observed in fluorocarbon elastomer,[51] and EPDM.[41] In addition, the trend observed in the 100% modulus with aging time was similarly reflected in the hardness test results. As the accelerated thermal aging temperature increased, the hardness values gradually rose, with a more pronounced rate of increase at higher temperatures. This increase in hardness indicates

15482634, 0, Downloaded from https://4spepublications.onlinelibrary.wiley.com/doi/10.1002/pen.27210 by Ecole De Technologie Superieur, Wiley Online Library on [23/04/2025]. See the Terms and Conditions (https://onlinelibrary.wiley.com/terms-and-conditions) on Wiley Online Library for rules of use; OA articles are governed by the applicable Creative Commons License

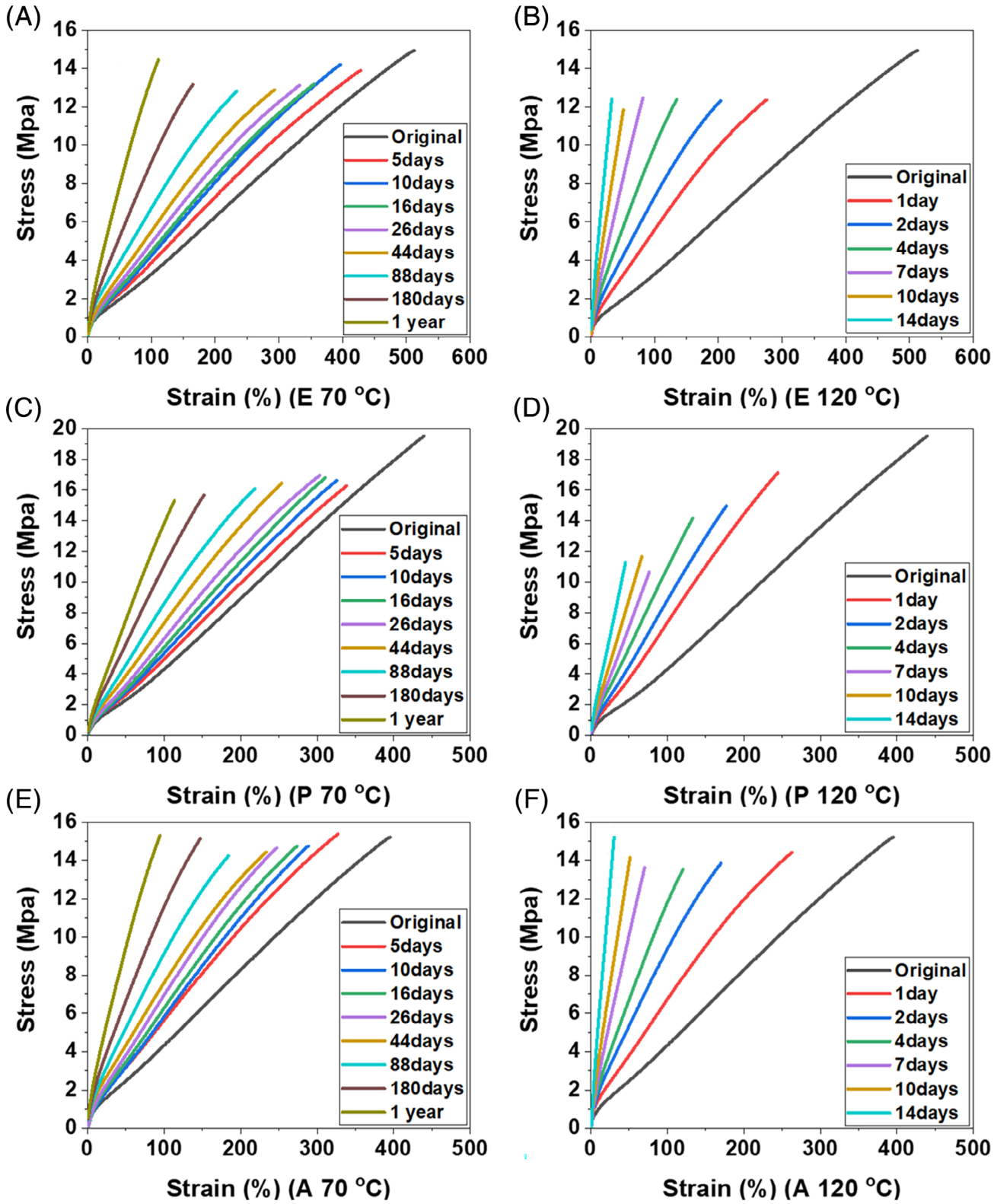

FIGURE 3 The stress–strain curves of tensile tests of the samples before and after aging for the lowest and highest temperatures under test at different times for: (A, B) E, (C, D) P, and (E, F) A samples.

greater stiffness in the compounds, likely due to cross-linking and the loss of low molecular weight materials not attached to the primary structure.

Overall, temperature plays a crucial role in this process. For instance, although 1 year at 70°C was required to achieve a 30%–40% change in 100% modulus for P, A, and E,

15482634, 0, Downloaded from https://4spepublications.onlinelibrary.wiley.com/doi/10.1002/pen.27210 by Ecole De Technologie Superieur, Wiley Online Library on [23/04/2025]. See the Terms and Conditions (https://onlinelibrary.wiley.com/terms-and-conditions) on Wiley Online Library for rules of use; OA articles are governed by the applicable Creative Commons License

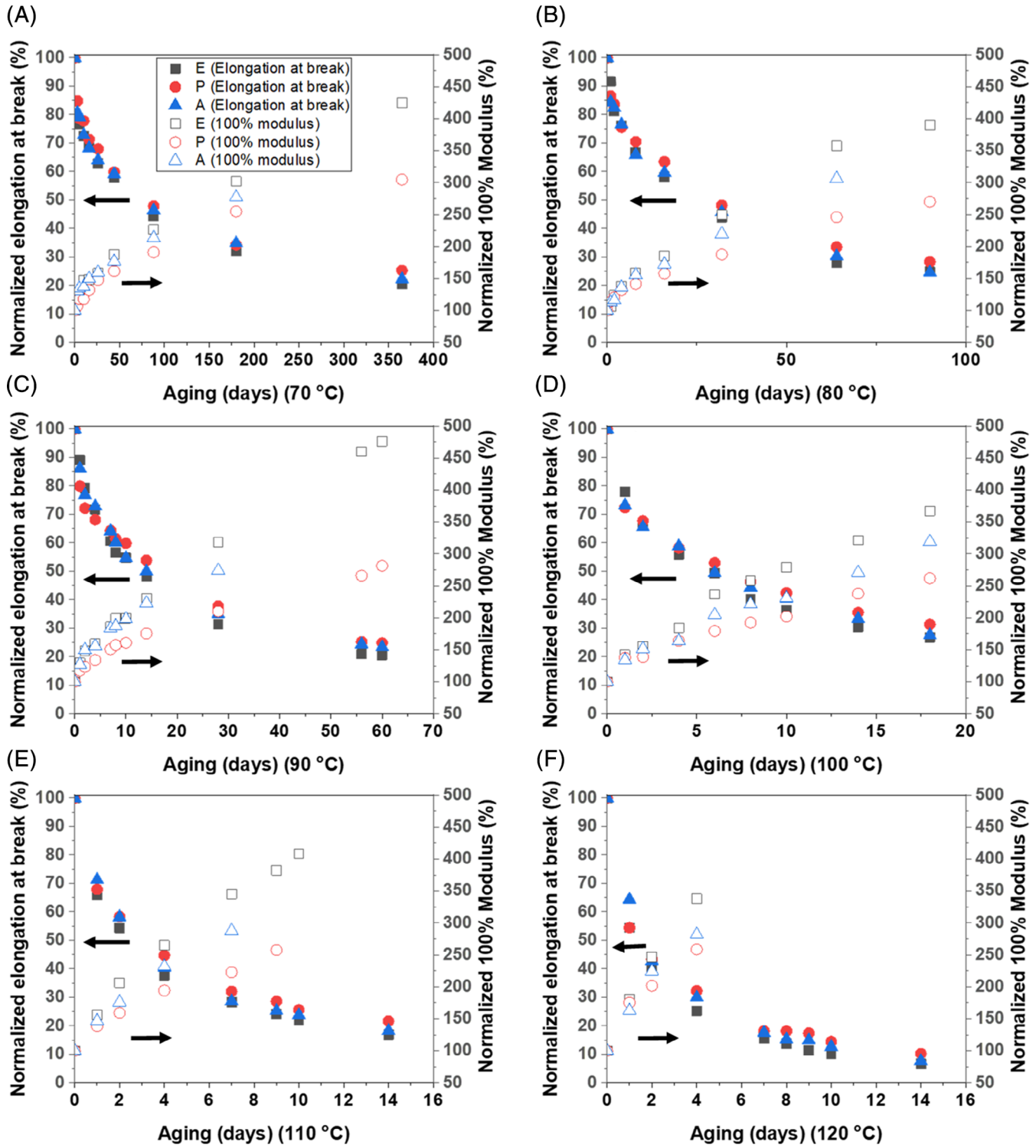

FIGURE 4 The normalized elongation at break and the 100% modulus versus aging time for the different temperatures: (A) 70, (B) 80, (C) 90, (D) 100, (E) 110, and (F) 120°C.

respectively, it took only about 8 days to reach the same change at 80°C. The hardening effect upon aging was also reported by others for fluorocarbon elastomer,[51] NBR,[52] and EPDM.[41]

For sample E, the changes in hardness were more significant compared to the other samples. This could be attributed to a higher proportion of unattached low molecular weight materials in its structure, which were prone to evaporation over time, leading to a more intense increase in hardness and 100% modulus. The other reason could be having a lower ratio of chain scission/cross-linking formation.

15482634, 0, Downloaded from https://4spepublications.onlinelibrary.wiley.com/doi/10.1002/pen.27210 by Ecole De Technologie Superieur, Wiley Online Library on [23/04/2025]. See the Terms and Conditions (https://onlinelibrary.wiley.com/terms-and-conditions) on Wiley Online Library for rules of use; OA articles are governed by the applicable Creative Commons License

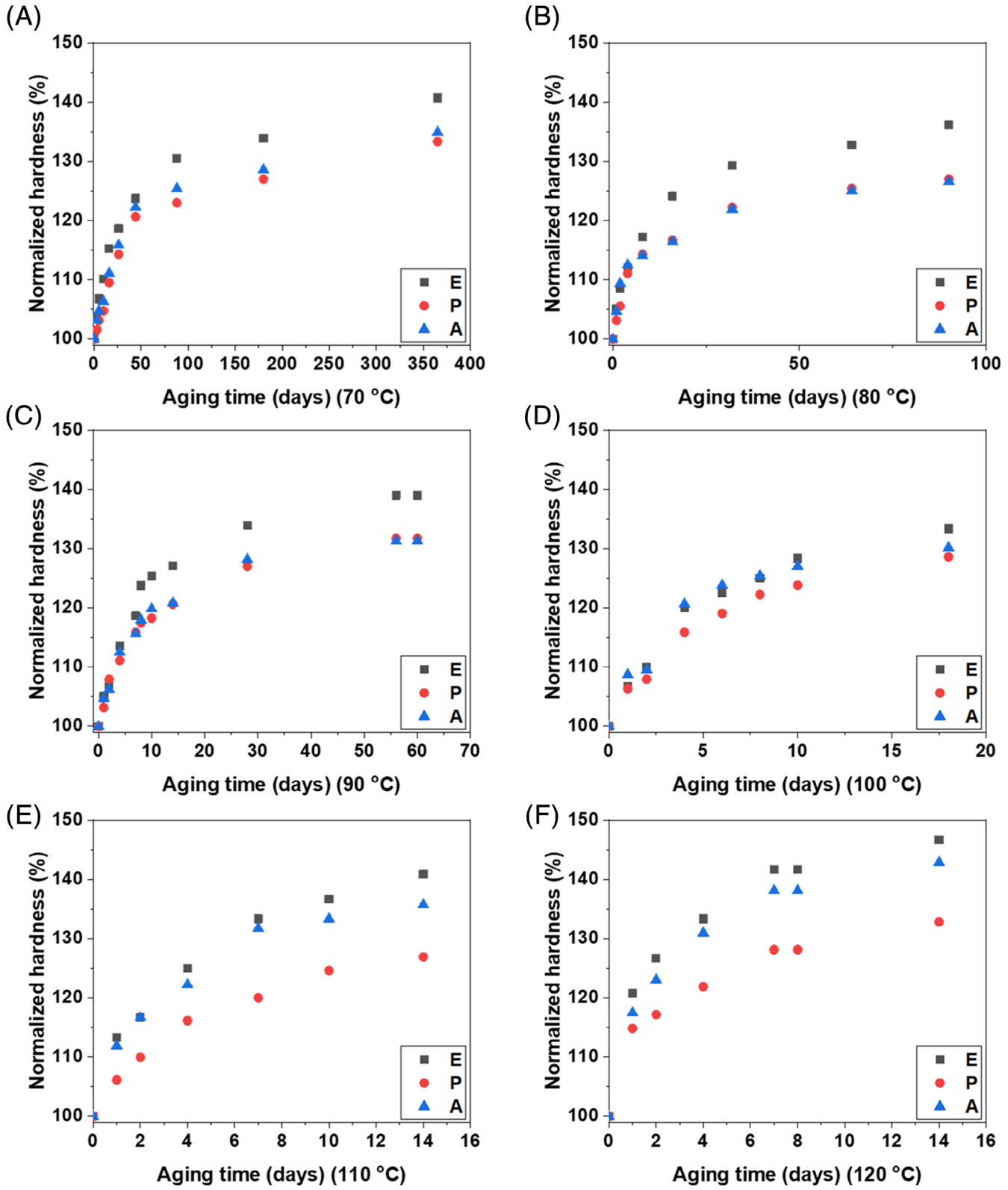

FIGURE 5 The normalized hardness versus aging time for the different temperatures: (A) 70, (B) 80, (C) 90, (D) 100, (E) 110, and (F) 120°C (some data points have been omitted for clarity).

In contrast, sample P exhibited less change in hardness for all temperatures from 100°C onward. Based on TGA results, the reason for the reduced change may be the lower percentage and the slower evaporation rate of the low molecular weight materials in its formulation, resulting in less migration to the surface and/or evaporation at

15482634, 0, Downloaded from https://4spepublications.onlinelibrary.wiley.com/doi/10.1002/pen.27210 by Ecole De Technologie Superieur, Wiley Online Library on [23/04/2025]. See the Terms and Conditions (https://onlinelibrary.wiley.com/terms-and-conditions) on Wiley Online Library for rules of use; OA articles are governed by the applicable Creative Commons License

TABLE 3 The results of the analysis of the change in network structure for the samples.

Sample	Temperature and time of aging	Weight swelling (%)	Dimension swelling (%)	Normalized weight swelling (%)	ρ_c ($\times 10^{-4}$ mol/cm^3)
E	Original sample	162.3 ± 0.3	203.9 ± 0.9	100.0 ± 0.2	1.3 ± 0.1
	70°C-88 days	115.4 ± 0.3	135.6 ± 3.0	71.1 ± 0.2	2.7 ± 0.1
	120°C-1 day	143.0 ± 0.4	173.7 ± 2.7	88.1 ± 0.2	1.9 ± 0.1
P	Original sample	160.3 ± 0.6	208.5 ± 2.0	100 ± 0.4	1.6 ± 0.1
	70°C-88 days	118.6 ± 0.4	156.3 ± 0.6	74.0 ± 0.1	2.7 ± 0.1
	120°C-1 day	125.2 ± 0.1	158.6 ± 0.8	78.1 ± 0.1	2.4 ± 0.1
A	Original sample	134.4 ± 0.1	165.8 ± 0.1	100 ± 0.1	1.9 ± 0.1
	70°C-88 days	101.1 ± 0.4	122.9 ± 3.1	75.2 ± 0.4	3.4 ± 0.1
	120°C-1 day	117.9 ± 0.6	148.6 ± 2.9	87.8 ± 0.5	2.6 ± 0.1

those temperatures. The reduced presence of low molecular weight materials means less evaporation, less material loss, and ultimately less change in the properties. It was seen that the weight reduction of P, A, and E upon aging for 1 day at 120°C was 1.83%, 4.20%, and 5.81%, respectively.

3.3 | Network structure analysis

To analyze the change in network structure, crosslink density, and the percentage of low molecular weight, the samples retaining nearly 50% elongation at break at different aging temperatures were cut to nearly the same dimensions, and they were immersed in toluene solvent. The results of the analysis of the change in network structure for the samples were tabulated in Table 3. As it is visible, the weight and dimension swelling reduced, so the calculated crosslink density increased upon aging of the samples. For example, in sample E, the weight and dimension swelling ratio of elastomer dropped from about 162 and 203 to about 115 and 135 for the sample aged at 70°C for 88 days, respectively. As it is shown, in normalized weight swelling, the weight swelling became about 71% of that of the original samples. These changes revealed that the aged samples had less capacity to absorb the solvent in their structure, and it is due to their higher crosslink density, which is about twofold that of the original samples, which is also tabulated in the table. The latter was due to the excess crosslinks produced upon the thermal aging. The increase in crosslink density and reduction in swelling percentage upon aging was also reported for SBR[13,14] CR,[53] and EPDM.[42]

3.4 | TGA results

TGA and weight loss rate (DTG) profiles of all the samples in the N_2 atmosphere are shown in Figure 6A,B,

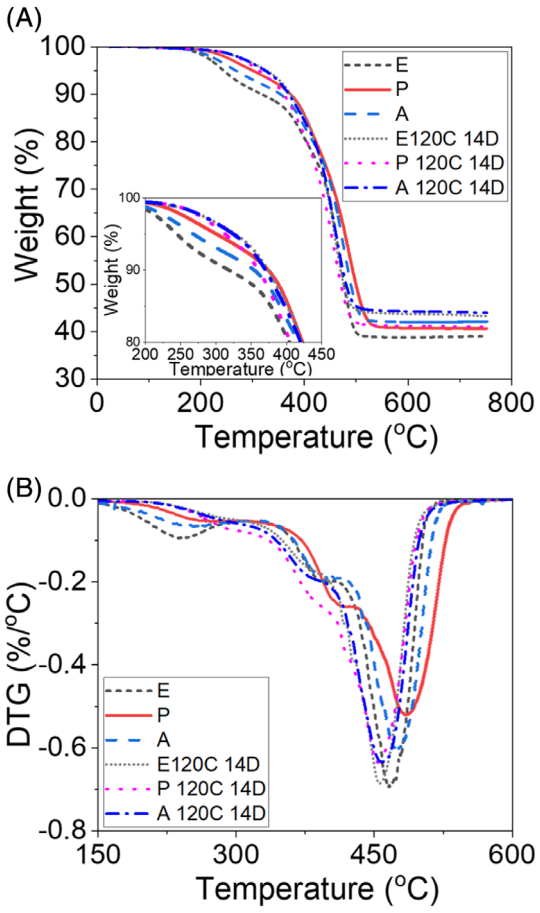

FIGURE 6 (A) TGA and (B) DTG curves for the materials in the N_2 atmosphere.

respectively. The materials exhibit two distinct mass loss steps. The first occurs between 200 and 400°C, likely due to the evaporation of low molecular weight components such as plasticizers, oils, and waxes. The second step, observed between 400 and 500°C, corresponds to polymer degradation.[54] There is a distinctive difference between

15482634, 0, Downloaded from https://4spepublications.onlinelibrary.wiley.com/doi/10.1002/pen.27210 by Ecole De Technologie Superieur, Wiley Online Library on [23/04/2025]. See the Terms and Conditions (https://onlinelibrary.wiley.com/terms-and-conditions) on Wiley Online Library for rules of use; OA articles are governed by the applicable Creative Commons License

the thermal decomposition behavior of three SBR-based samples, especially in the first step. As observed from the TGA curve, the thermal stability of the samples increases in the order: E, A, and P, as it is visible in the inset image of Figure 6A. It is an indication of higher low molecular materials that it has in its structure. In addition, it is seen that the residual of the samples was not the same for unaged samples, and as calculated and reported in Table 1, the percentage of carbon black was not the same for the samples. It has been reported that both mass loss steps can also be influenced by the amount of carbon black present. Hence, it can also be considered an important affecting factor on the thermal stability of the materials.[54]

The corresponding DTG of the sample showed three peaks, in which the peaks are much more intense, which correspond to the highest material degradation in the order: E, A, and P. Each degradation peak happened because of different component degradations. The lower temperature degradations can be related to the degradation of low molecular weight materials that do not withstand higher temperatures and therefore decompose at lower temperatures. Based on the analysis, sample E has the highest amount of low molecular weight in its system, followed by A and P samples, respectively.

For the aged samples, it was observed that the first step of degradation had nearly disappeared. Additionally, the materials exhibited higher thermal stability, as evidenced by increased T10% values and higher residual mass. It was also reported in another work, and it was related to limited oxygen diffusion due to the increased network density.[17] However, it is important to account for the evaporation of certain components during the aging process, as observed in some samples by comparing their weights before and after aging. This evaporation likely contributed to the increased thermal stability and residual mass. The reduction in low molecular weight components due to evaporation resulted in a relatively higher proportion of more stable components.

The DTG results further showed that the two initial peaks at lower temperatures either disappeared or became less pronounced, forming a shoulder. This indicates that a portion of the material originally present no longer exists in the aged samples. Similar findings, such as lower DTG peaks and T_{max} after aging, have also been reported for SBR in another work and attributed to structural modifications caused by thermal aging, including the formation of macromolecular radicals and oxygenated species which are weak points.[17]

3.5 | Lifetime prediction

The Arrhenius method can be used to predict the lifetime of material at other temperatures. The time to reach the criteria of a 50% reduction in normalized elongation at break was considered the degradation time to predict the service time of the samples. To obtain the time needed to reach a 50% reduction in elongation at break and a 50% augmentation in 100% modulus, extrapolation was done to the data obtained for the normalized elongation at break and 100% modulus, which were depicted in Figure 4.

Then, the curve of Ln(t) versus $1/T$ for t at which 50% of reduction in elongation at break and 100% modulus were depicted in Figure 7. Based on ISO 11346, the highest temperature should be chosen to ensure that the time required to meet the criteria is at least 100 h. For temperatures higher than 100°C, the samples degrade faster than 100 h; therefore, the data were not suitable to be used for lifetime prediction. Therefore, we have used 70–100 and also 70–120°C to find out their effects on the lifetime prediction.

The data and equation obtained from fitting the curve of Ln(t) as a function of $1/T$, where t represents the time at which a 50% change in either elongation at break or 100% modulus was recorded, are presented in Table 4. To calculate the parameters and prediction of the life, Origin 2019 software was used in this work. As can be seen, the absolute value of activation energy and lifetime were higher in order of P, E, and A, respectively, for both temperature ranges of 100% modulus and the temperature range of 70–120°C for elongation at break. However, for elongation at break within the range of 70–100°C, the values were nearly identical. Furthermore, the lifetimes obtained from elongation at break and 100% modulus were not the same, which was reasonable since their rates of change with temperature differ.

In the literature, it is mentioned that in the accelerated degradation of polymer and rubber, the degradation can be affected by diffusion-limited oxidation (DLO). DLO means that oxygen diffusion is limited upon thermal aging. This leads to the heterogeneous oxidation phenomenon, adding to the complexity of the aging process. This effect becomes more pronounced with increasing thermal aging temperature and sample thickness.[55,56] However, in this work, for both properties across both temperature ranges, the R^2 values were high, and the data followed the Arrhenius equation. This could be due to the excessive thickness of the samples, which was sufficient to prevent heterogeneous degradation caused by the DLO effect. Meanwhile, it is also evident that altering the temperature range in the Arrhenius methodology can significantly impact the predicted lifetime. This is because the methodology relies on a single data point for each temperature, making it less reliable.

Another methodology that can be used to predict the lifetime of the elastomers is TTS. As the elongation at

15482634, 0, Downloaded from https://4spepublications.onlinelibrary.wiley.com/doi/10.1002/pen.27210 by Ecole De Technologie Superieur, Wiley Online Library on [23/04/2025]. See the Terms and Conditions (https://onlinelibrary.wiley.com/terms-and-conditions) on Wiley Online Library for rules of use; OA articles are governed by the applicable Creative Commons License

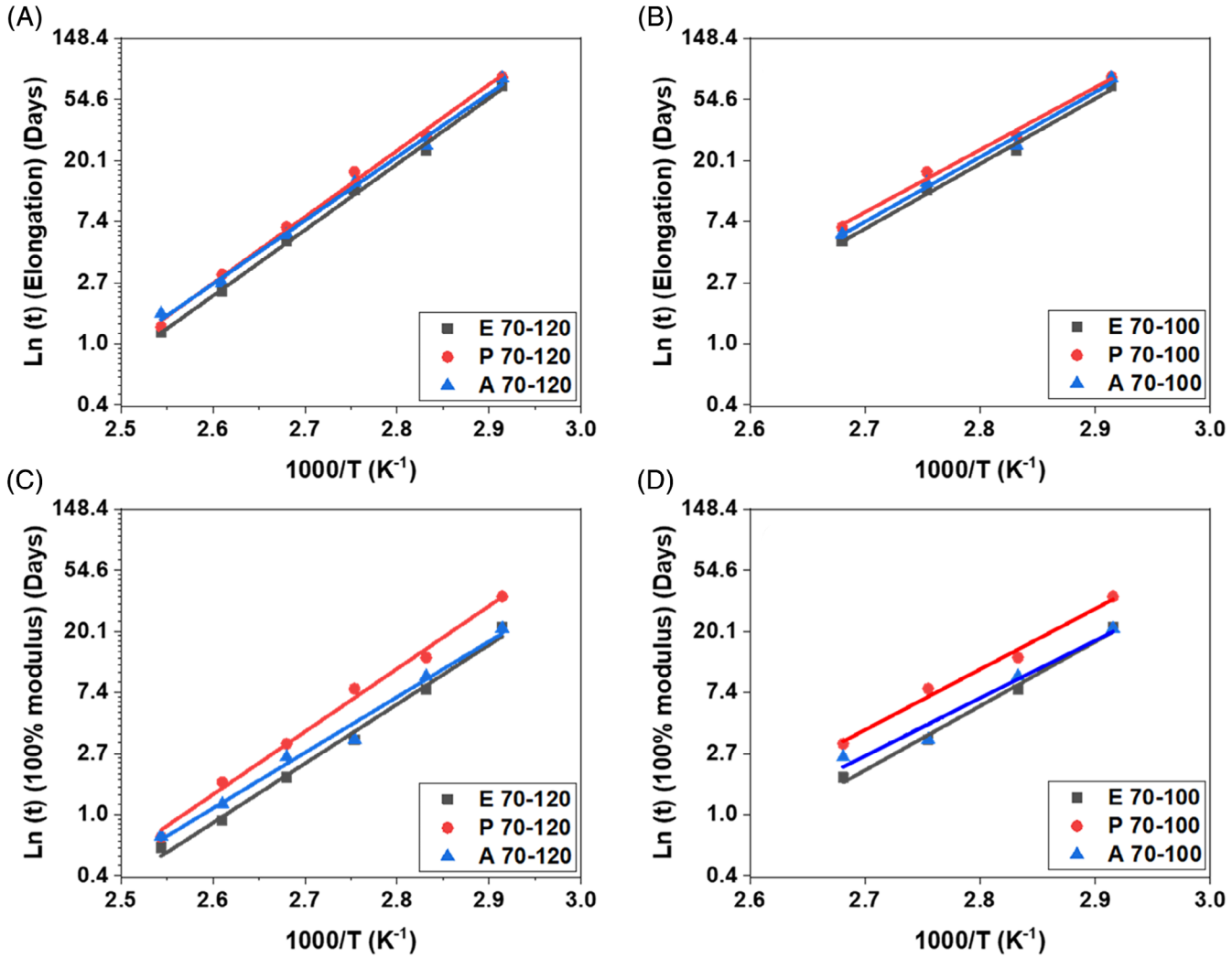

FIGURE 7 The curve of Ln(t) versus $1/T$ for t at which 50% of the change in elongation at break for the temperature range of (A) 70–120°C, (B) 70–100°C, and 100% modulus for the temperature range of (C) 70–120°C (D) 70–100°C.

break is well established that it can produce much better lifetime prediction,[57] only elongation at break data were used for been estimated by this method. To apply the methodology, first, the curves of the normalized elongation at break versus the accelerated thermal aging time must be plotted for all the temperatures under study as depicted in Figure 8. Then, the data should be shifted in time axe using an empirical shifting factor so that the data obtained from each temperature superpose on each other, Figure 8. Once the shifted factors are found, the logarithmic plot of shifting factors versus the inverse of their corresponding temperature ranged from 70 to 120°C can be traced as in Figure 9. By fitting the curve using the linear curve fitting method, the equation can be calculated as well as activation energy. Therefore, the shifting factor in the other temperatures can be extrapolated. Having the shifting factor, the TTS curve could be plotted at the desired temperature using the data from 70 to 120°C, Figure 9. With that, the time in which 50% of the change in the elongation at break is predicted to happen can be calculated.

At temperatures above 100°C, the samples degrade too quickly, less than 100 h, making the data unsuitable for lifetime prediction according to ISO 11346. The logarithmic plot of shifting factors versus the inverse of their corresponding temperature and the TTS curve could also be plotted for 70–100°C, as shown in Figure 10. As the slope of the prediction line for the plot of shifting factors versus the inverse of their corresponding temperature is different for the temperature range of 70–100°C in comparison with that of 70–120°C, the ambient temperature shift factors obtained for 23°C from these two temperature ranges were also different from each other. Consequently, the prediction time would also be different.

15482634, 0, Downloaded from https://4spepublications.onlinelibrary.wiley.com/doi/10.1002/pen.27210 by Ecole De Technologie Superieur, Wiley Online Library on [23/04/2025]. See the Terms and Conditions (https://onlinelibrary.wiley.com/terms-and-conditions) on Wiley Online Library for rules of use; OA articles are governed by the applicable Creative Commons License

TABLE 4 The equations were obtained by fitting the equation of the curve of Ln(t) versus $1/T$.

Property	Temperature ranged used	Equation	$y = a + b \times x$, where Y is Ln(t) and X is $1/T$		
			P	E	A
Elongation at break	70–120°C	a	−27.2	−27.2	−26.0
		b	10,843	10,773	10,380
		Adj. R^2	0.995	0.997	0.994
		E_a	−90.2	−89.6	−86.3
		Lifetime at 23°C (years)	34	26	23
Elongation at break	70–100°C	a	−25.4	−26.8	−26.6
		b	10,200	10,631	10,599
		Adj. R^2	0.989	0.991	0.985
		E_a	−84.8	−88.4	−88.1
		Lifetime at 23°C (years)	24	24	26
100% modulus	70–120°C	a	−26.4	−25.4	−23.56
		b	10,283	9700	9103
		Adj. R^2	0.989	0.988	0.989
		E_a	−85.5	−80.6	−75.7
		Lifetime at 23°C (years)	11	5	4
100% modulus	70–100°C	a	−25.4	−27.6	−24.5
		b	9905	10,507	9443
		Adj. R^2	0.981	0.989	0.951
		E_a	−82.4	−87.4	−78.5
		Lifetime at 23°C (years)	9	7	4

The equations obtained from fitting the TTS curves are presented in Table 5. As can be seen, the equation obtained for 70–100°C was less complex in comparison to that of 70–130°C. It could be related to the fact that for higher temperatures other mechanisms of degradation like chain scission intervened and made the data and their prediction much more complex. It should be noted that three-phase and two-phase exponential decay functions were estimated for all samples, considering the temperature ranges of 70–120 and 70–100°C, respectively. Adjusted R^2 (Adj. R^2) for all samples considering 70–120 and for 70–100°C was higher than 0.991 and 0.983, respectively. In terms of lifetime prediction, it was observed that the temperature range did not significantly affect the predictions, and the lifetimes obtained for each material were distinctly different. This may be attributed to the fact that this method utilizes all the data points obtained for each temperature. Therefore, it seems that the TTS method is much more reliable than the Arrhenius method to predict lifetime. The highest lifetimes were observed in the order of P, A, and E. However, these predictions provide valuable insight into the long-term stability of the materials; it is important to acknowledge the inherent uncertainties in such estimations. Factors such as environmental variations, mechanical stresses, and potential deviations from the assumed degradation mechanisms could influence actual service lifetimes. Additionally, the extrapolation process assumes that the degradation kinetics observed in accelerated conditions remain consistent over extended periods, which may not fully capture real-world aging effects. Therefore, while the predicted lifetimes serve as reasonable projections, they should be interpreted as indicative estimates rather than absolute values. Future studies incorporating real-time aging data and broader environmental conditions would further validate and refine these predictions.

To wrap up the results, it should be noted that the aging mechanism of the SBR-based elastomeric samples primarily resulted in increased hardness and brittleness, as evidenced by mechanical test results. This phenomenon can be attributed to two key degradation processes: crosslinking and the loss of low molecular weight components. The increase in crosslink density upon thermal aging was confirmed by swelling tests. This indicates that oxidation and recombination reactions led to the formation of additional crosslinks

15482634, 0, Downloaded from https://4spepublications.onlinelibrary.wiley.com/doi/10.1002/pen.27210 by Ecole De Technologie Superieur, Wiley Online Library on [23/04/2025]. See the Terms and Conditions (https://onlinelibrary.wiley.com/terms-and-conditions) on Wiley Online Library for rules of use; OA articles are governed by the applicable Creative Commons License

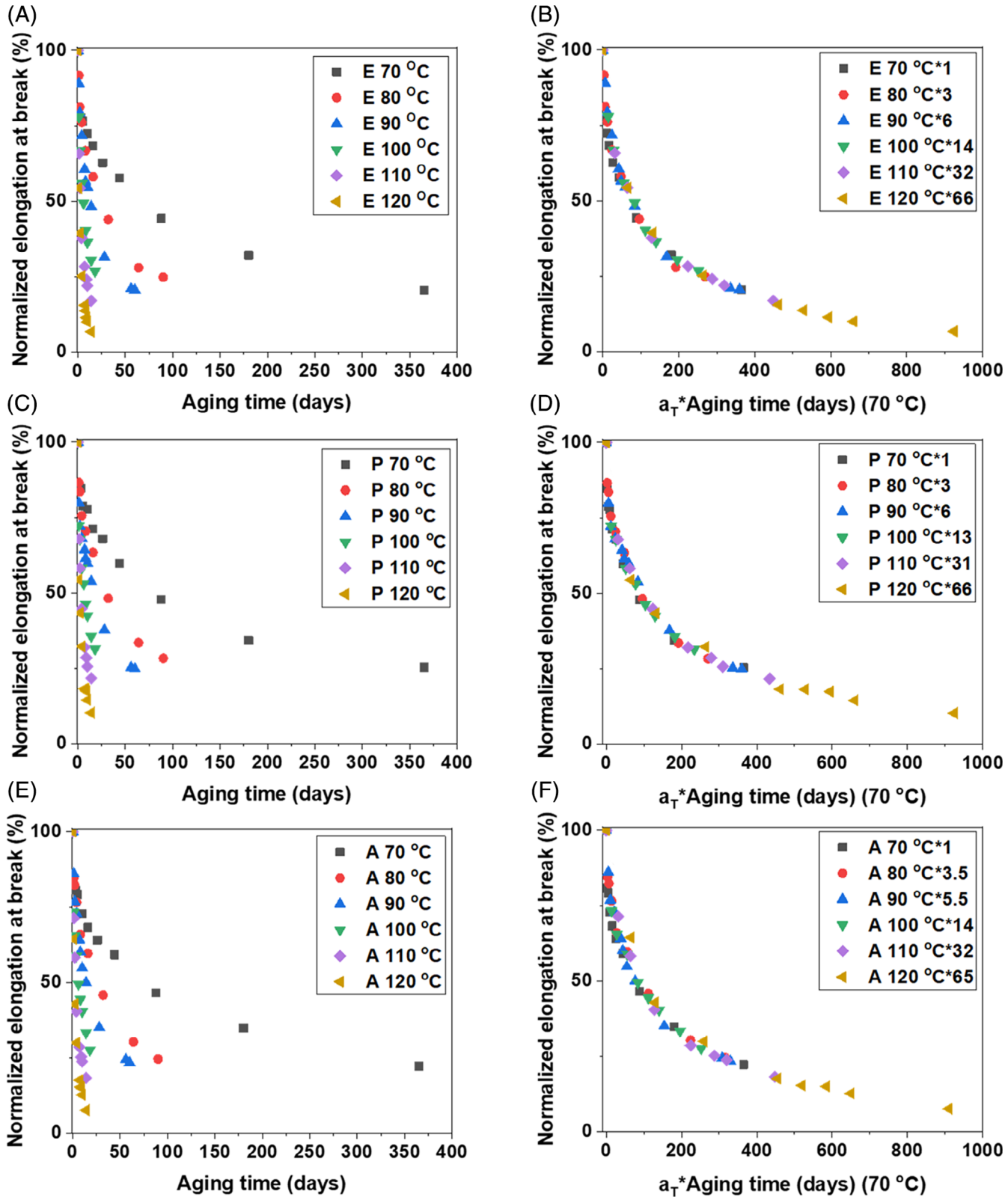

FIGURE 8 The curves of the normalized elongation at break versus the aging time at the temperatures under study and their corresponding master curve for 70°C for sample E (A, B), sample P (C, D), and sample A (E, F).

within the polymer network. As the material aged, these additional crosslinks reduced the mobility of the polymer chains, making the elastomer stiffer and less flexible, ultimately leading to embrittlement. Furthermore, thermogravimetric analysis (TGA) and weight loss measurements demonstrated a measurable

15482634, 0, Downloaded from https://4spepublications.onlinelibrary.wiley.com/doi/10.1002/pen.27210 by Ecole De Technologie Superieur, Wiley Online Library on [23/04/2025]. See the Terms and Conditions (https://onlinelibrary.wiley.com/terms-and-conditions) on Wiley Online Library for rules of use; OA articles are governed by the applicable Creative Commons License

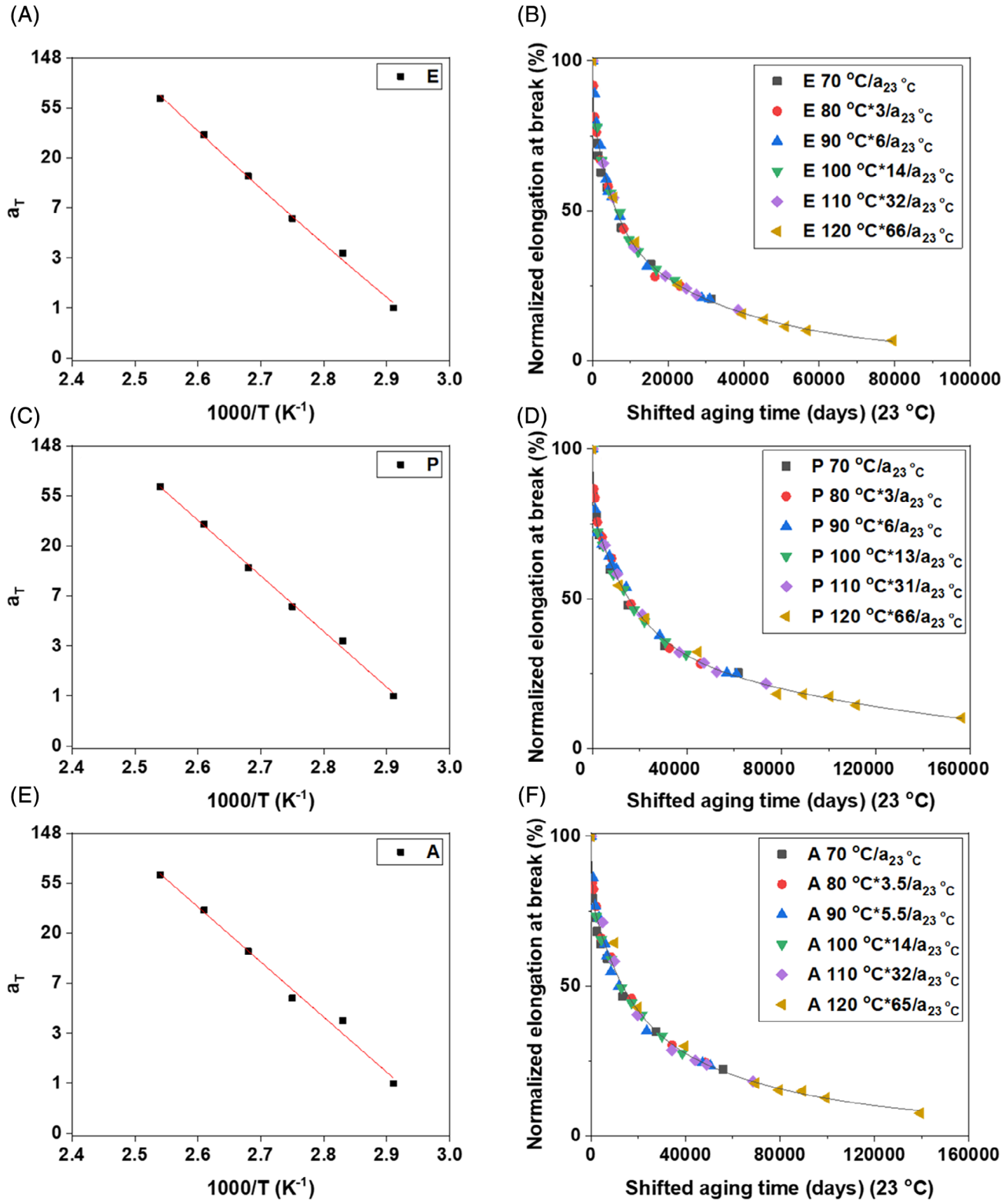

FIGURE 9 The logarithmic plot of shifting factors of elongation at break versus the inverse of their corresponding temperature in the range of 70–120°C and their resultant TTS curves of samples for 23°C for sample E (A, B), sample P (C, D) and sample A (E, F).

reduction in mass due to the evaporation of low molecular weight additives and volatile degradation byproducts. These components, often added to improve processing and mechanical properties, tend to evaporate at elevated temperatures, further contributing to the observed increase in hardness and reduction in elongation at break. Additionally, oxidation reactions occurring at high temperatures may have played a role in structural degradation.

15482634, 0, Downloaded from https://4spepublications.onlinelibrary.wiley.com/doi/10.1002/pen.27210 by Ecole De Technologie Superieur, Wiley Online Library on [23/04/2025]. See the Terms and Conditions (https://onlinelibrary.wiley.com/terms-and-conditions) on Wiley Online Library for rules of use; OA articles are governed by the applicable Creative Commons License

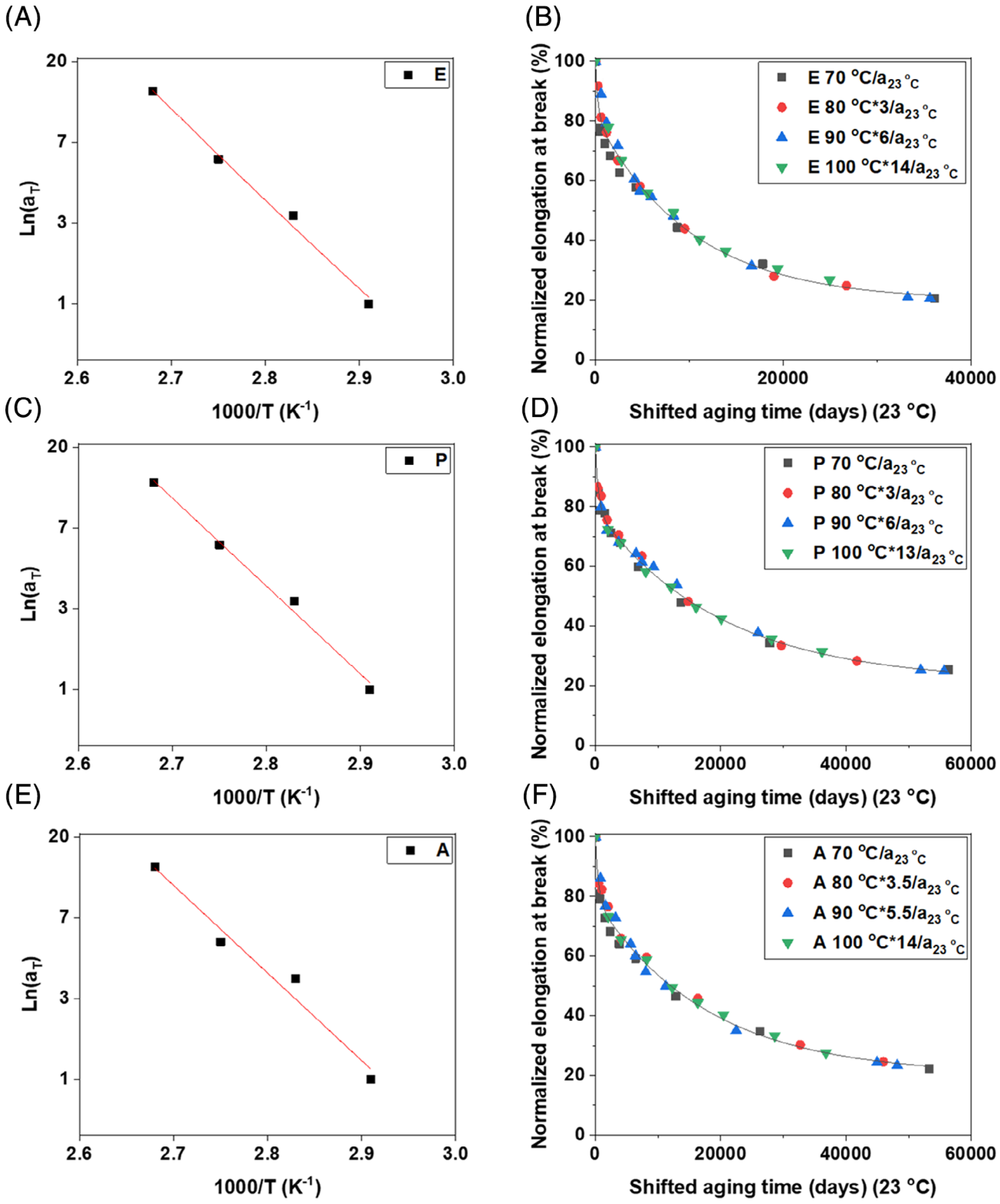

FIGURE 10 The logarithmic plot of shifting factors of elongation at break versus the inverse of their corresponding temperature in the range of 70–100°C and their resultant TTS curves of samples for 23°C for sample E (A, B), sample P (C, D), and sample A (E, F).

Thermo-oxidative aging can induce chain scission, particularly at higher temperatures, which competes with crosslink formation.

To understand the change in the aging mechanism of SBR composites, an Ahagon plot[58] can be utilized, which is a logarithmic plot of elongation at break versus 100%

15482634, 0, Downloaded from https://4spepublications.onlinelibrary.wiley.com/doi/10.1002/pen.27210 by Ecole De Technologie Superieur, Wiley Online Library on [23/04/2025]. See the Terms and Conditions (https://onlinelibrary.wiley.com/terms-and-conditions) on Wiley Online Library for rules of use; OA articles are governed by the applicable Creative Commons License

TABLE 5 The equations were obtained from the fitting of TTS curves.

Property and temperature ranged used	Equation	$y = a_1$*exp$(-x/t_1) + a_2$*exp$(-x/t_2) + a_3$*exp$(-x/t_3) + y0$, where Y is normalized elongation at break and X is time		
		P	E	A
Elongation at break 70–120°C	$a_{23°C}$	5.91×10^{-3}	11.63×10^{-3}	6.53×10^{-3}
	y_0	−3.8	1.75	3.41
	a_1	42.5	16.1	40.3
	t_1	16,905	168	66,981
	a_2	20.6	38.5	20.0
	t_2	540	5259	452
	a_3	40.7	43.6	36.2
	t_3	144,683	35,224	13,729
	Adj. R^2	0.997	0.991	0.991
	Lifetime at 23°C (50% elongation) (years)	42	17	34
Elongation at break 70–100°C	$a_{23°C}$	6.47×10^{-3}	10.11×10^{-3}	6.85×10^{-3}
	y_0	21.3	19.7	20.2
	a_1	21.0	18.4	20.8
	t_1	516	280	502
	a_2	57.6	61.7	58.8
	t_2	19,916	10,176	17,769
	a_3	-	-	-
	t_3	-	-	-
	Adj. R^2	0.995	0.983	0.990
	Lifetime at 23°C (50% elongation) (years)	38	20	37

Modulus, Figure 11. This plot can reveal three different degradation mechanisms:

- Type I: The modulus increases while the elongation at break decreases, primarily due to crosslinking as the dominant mechanism.
- Type II: A slight change or reduction in modulus is observed, along with a decrease in elongation at break, typically under anaerobic aging conditions.
- Type III: The modulus increases, and the elongation at break significantly decreases due to a combination of chain scission and crosslinking reactions, particularly under oxidative aging conditions.[1,58]

However, in this work, only Types I and III have been seen. The area in which the slope was about −0.8 means that SBR composites degradation was the type I, which means that the crosslinking mechanism was predominant. For the accelerated thermal aging temperatures of 70–90°C, the data belonging to the early days of aging lie on these lines. This indicated the crosslinking reactions are superior in that region. The remaining data lie on lines with higher slopes, about 1.15 and higher, related to the type III mechanism. This type of degradation was characterized by mostly scission reactions.[58] The degradation can be described as a process where oxygen exposure leads to the formation of a hydroperoxide molecule. This hydroperoxide then breaks down into highly reactive free radicals, which set off a chain reaction of further breakdowns. Antioxidants can slow this process by capturing some of these free radicals. However, as the antioxidants are used up over time and with increasing heat, the free radicals continue to be generated and promote the breakdown of the compound. This suggests that at elevated temperatures as well as prolonged aging, this chain scission process becomes the dominant force. This approach has also been employed by other researchers to investigate the aging mechanisms.[59,60] The presence of only the two aforementioned mechanisms has also been observed in natural rubber (NR).[61] In summary, the thermal aging mechanism of these SBR elastomers was primarily governed by

15482634, 0, Downloaded from https://4spepublications.onlinelibrary.wiley.com/doi/10.1002/pen.27210 by Ecole De Technologie Superieur, Wiley Online Library on [23/04/2025]. See the Terms and Conditions (https://onlinelibrary.wiley.com/terms-and-conditions) on Wiley Online Library for rules of use; OA articles are governed by the applicable Creative Commons License

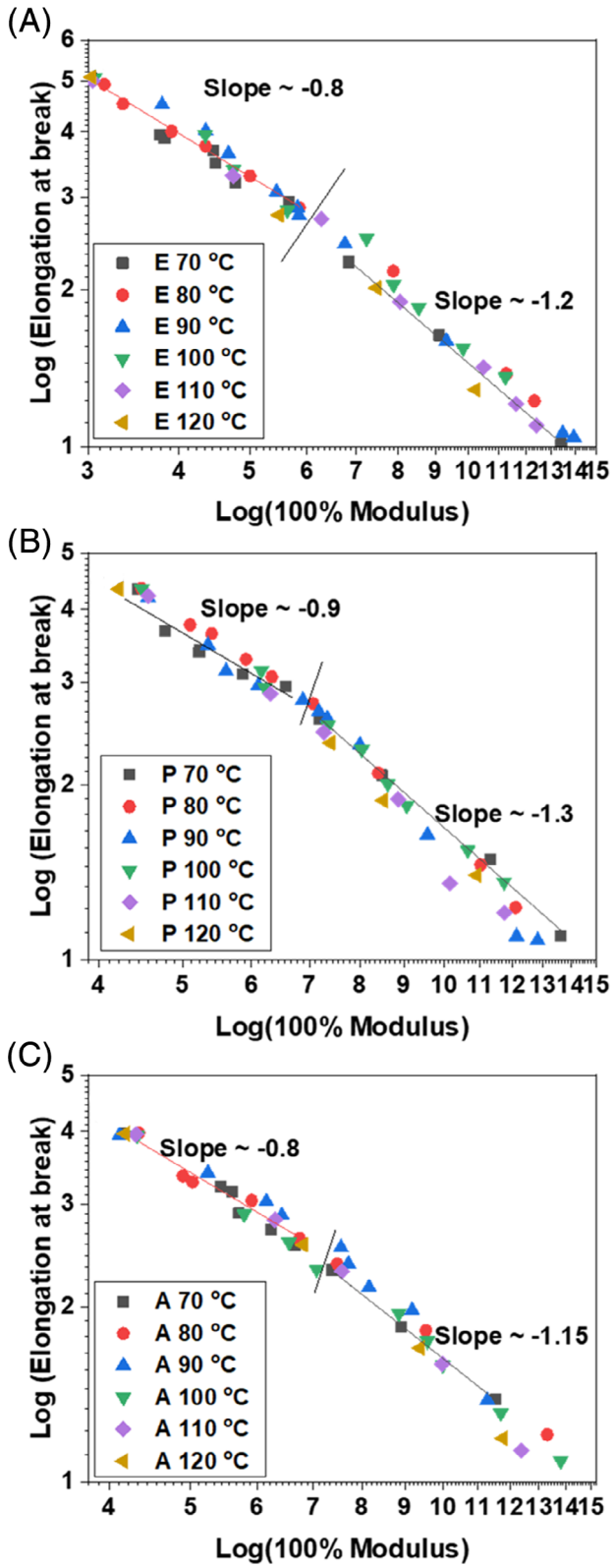

FIGURE 11 Ahagon plot for the samples under test for E, P, and A.

crosslinking-induced stiffening and the volatilization of low molecular weight species, both of which led to a decline in mechanical performance over time.

4 | CONCLUSION

This study investigated the thermal aging behavior of three SBR-based elastomeric compounds containing carbon black. The thermo-oxidative aging process was carried out at temperatures ranging from 70 to 120°C for various durations, from 14 to 365 days. The results of the tensile and hardness tests on aged samples showed that hardness and the 100% modulus increased, while elongation at break decreased for all three samples. These changes were temperature-dependent, with higher temperatures accelerating degradation. For example, at 70°C, a reduction of approximately 50% in elongation at break was observed in less than 90 days for all three samples, whereas at 120°C, this same level of degradation occurred in under 2 days. This behavior can be attributed to an increase in crosslink density and the evaporation of low molecular weight material upon aging, as evidenced by swelling tests and weight measurements before and after aging.

Swelling tests confirmed an increase in crosslink formation in the SBR elastomer over time. Additionally, laser microscopy was used to analyze microstructural changes, revealing the formation of surface roughness and other defects. These findings indicate degradation processes such as oxidation, crosslinking, and the evaporation of low molecular weight components.

To predict the lifetime of these materials, both the Arrhenius method and time–temperature superposition (TTS) were evaluated. The TTS method was found to provide more accurate predictions as it utilizes all available data, whereas the Arrhenius method relies on only one data point per temperature. Furthermore, by comparing the two temperature intervals using an Ahagon plot, it was observed that at higher temperatures, the degradation mechanism shifted, with chain scission becoming predominant.

For future work, improving lifetime predictions by considering a broader range of environmental factors would enhance accuracy. Investigating the combined effects of ozone exposure and thermal aging could provide deeper insights into material degradation mechanisms. Additionally, studying the simultaneous influence of compression and heat on the samples could offer a more realistic assessment of their long-term performance.

ACKNOWLEDGMENTS

The authors would like to thank the following granting agencies: Natural Sciences and Engineering Research Council of Canada (NSERC), Prima-Quebec, Canada; Hydro-Québec, Canada, and Helix-Canada for their financial support for this work. Special thanks to technicians and students who have helped us complete this project.

15482634, 0, Downloaded from https://4spepublications.onlinelibrary.wiley.com/doi/10.1002/pen.27210 by Ecole De Technologie Superieur, Wiley Online Library on [23/04/2025]. See the Terms and Conditions (https://onlinelibrary.wiley.com/terms-and-conditions) on Wiley Online Library for rules of use; OA articles are governed by the applicable Creative Commons License

CONFLICT OF INTEREST STATEMENT

The authors declare no conflicts of interest.

DATA AVAILABILITY STATEMENT

Data available on request due to privacy/ethical restrictions.

ORCID

Said Elkoun https://orcid.org/0000-0003-0501-6872
Phuong Nguyen-Tri https://orcid.org/0000-0001-6578-5716

REFERENCES

1. Tayefi M, Eesaee M, Hassanipour M, Elkoun S, David E, Nguyen-Tri P. Recent progress in the accelerated aging and lifetime prediction of elastomers: a review. *Polym Degrad Stab*. 2023;214:110379. doi:10.1016/j.polymdegradstab.2023.110379
2. Simpson RB. *Rubber Basics*. Rapra Technology Limited; 2002: 77-89.
3. Nguyen-Tri P, Triki E, Nguyen TA. Butyl rubber-based composite: thermal degradation and prediction of service lifetime. *J Compos Sci*. 2019;3:48. doi:10.3390/jcs3020048
4. El Aidani R, Nguyen-Tri P, Malajati Y, Lara J, Vu-Khanh T. Photochemical aging of an e-PTFE/NOMEX® membrane used in firefighter protective clothing. *Polym Degrad Stab*. 2013; 98(7):1300-1310. doi:10.1016/j.polymdegradstab.2013.04.002
5. Nguyen- Tri P, El Aidani R, Leborgne É, Pham T, Vu-Khanh T. Chemical aging of a polyester nonwoven membrane used in aerosol and drainage filter. *Polym Degrad Stab*. 2014;101:71-80. doi:10.1016/j.polymdegradstab.2014.01.001
6. Nguyen TV, Nguyen TP, Nguyen TD, El Aidani R, Trinh VT, Decker C. Accelerated degradation of water borne acrylic nanocomposites used in outdoor protective coatings. *Polym Degrad Stab*. 2016;128:65-76. doi:10.1016/j.polymdegradstab.2016.03.002
7. Bui TMA, Nguyen TV, Nguyen TM, et al. Investigation of crosslinking, mechanical properties and weathering stability of acrylic polyurethane coating reinforced by SiO_2 nanoparticles issued from rice husk ash. *Mater Chem Phys*. 2020;241: 122445. doi:10.1016/j.matchemphys.2019.122445
8. Qian C, Li Y, Zhao J, Wang S, He E. Thermal-oxidative aging and tribological properties of carbon nanotube/nitrile butadiene rubber composites with varying acrylonitrile content: molecular dynamics simulations. *Polym Eng Sci*. 2023;63(5): 1516-1527. doi:10.1002/pen.26302
9. Song M, Wang M, Wang C, et al. Molecular simulation and experimental study on the damping and aging properties of 4010NA/hydrogenated nitrile butadiene/nitrile butadiene rubber composites. *Macromol Theory Simul*. 2023;32(2):2370003. doi:10.1002/mats.202370003
10. Zhao J, Yu M, Qian C, Wang S, Wang Z. Thermal-oxidative aging behavior of graphene and graphene oxide-filled nitrile butadiene rubber: a molecular simulation approach. *Polym Eng Sci*. 2023;63(2):660-671. doi:10.1002/pen.26238
11. Wang S, Wang C, He A. Accelerated aging behavior and degradation mechanism of nitrile rubber in thermal air and hydraulic oil environments. *Polymr Eng Sci*. 2023;63(7):2218-2232. doi: 10.1002/pen.26371
12. de Souza EL, de Sousa Zanzi M, de Paiva KV, Oliveira JLG, de Oliveira Barra GM, Dutra GB. Thermo-oxidative aging of acrylonitrile–butadiene rubber gaskets with real geometry used in plate heat exchangers. *J Appl Polym Sci*. 2023;140(5):e53419. doi:10.1002/app.53419
13. Maciejewska M, Zaborski M. Ionic liquids as coagents for sulfur vulcanization of butadiene–styrene elastomer filled with carbon black. *Polym Bull*. 2018;75(10):4499-4514. doi:10.1007/s00289-018-2281-6
14. Rezig N, Bellahcene T, Aberkane M, Nait Abdelaziz M. Thermo-oxidative ageing of a SBR rubber: effects on mechanical and chemical properties. *J Polym Res*. 2020;27:1-13. doi:10.1007/s10965-020-02330-y
15. Guo L, Huang G, Zheng J, Li G. Thermal oxidative degradation of styrene–butadiene rubber (SBR) studied by 2D correlation analysis and kinetic analysis. *J Thermal Anal Calor*. 2014;115: 647-657. doi:10.1007/s10973-013-3348-0
16. Ghosh J, Ghorai S, Bhunia S, Roy M, De D. The role of devulcanizing agent for mechanochemical devulcanization of styrene butadiene rubber vulcanizate. *Polym Eng Sci*. 2017; 58(1):74-85. doi:10.1002/pen.24533
17. Xiang K, Wang X, Huang G, Zheng J, Huang J, Li G. Thermogravimetric studies of styrene–butadiene rubber (SBR) after accelerated thermal aging. *J Thermal Anal Calor*. 2014;115:247-254. doi:10.1007/s10973-013-3236-7
18. Xiang K, Wang X, Huang G, Zheng J, Huang J, Li G. Thermal ageing behavior of styrene–butadiene random copolymer: a study on the ageing mechanism and relaxation properties. *Polym Degrad Stab*. 2012;97:1704-1715. doi:10.1016/j.polymdegradstab.2012.06.015
19. Choi SS, Kim JC. Lifetime prediction and thermal aging behaviors of SBR and NBR composites using crosslink density changes. *J Ind Eng Chem*. 2012;18(3):1166-1170. doi:10.1016/j.jiec.2012.01.011
20. Mostafa A, Abouel-Kasem A, Bayoumi MR, El-Sebaie MG. The influence of CB loading on thermal aging resistance of SBR and NBR rubber compounds under different aging temperature. *Mater Des*. 2009;30:791-795. doi:10.1016/j.matdes.2008.05.065
21. Kim DY, Park JW, Lee DY, Seo KH. Correlation between the crosslink characteristics and mechanical properties of natural rubber compound via accelerators and reinforcement. *Polymers (Basel)*. 2020;12(9):12092020. doi:10.3390/polym12092020
22. Madeira H, Gac P-YL, Gall ML, Verron E. Impact of carbon black content in relationships between mechanical properties and crosslinking of filled polychloroprene during oxidative aging. *Rubber Chem Technol*. 2025;98(1):46-61. doi:10.5254/rct.24.00026
23. Kömmling A, Jaunich M, Goral M, Wolff D. Insights for lifetime predictions of O-ring seals from five-year long-term aging tests. *Polym Degrad Stab*. 2020;179:109278. doi:10.1016/j.polymdegradstab.2020.109278
24. Kömmling A, Jaunich M, Pourmand P, Wolff D, Gedde UW. Influence of ageing on sealability of elastomeric O-rings. *Macromol Symp*. 2017;373(1):1600157. doi:10.1002/masy.201600157
25. Kömmling A, Jaunich M, Wolff D. Revealing effects of chain scission during ageing of EPDM rubber using relaxation and recovery experiment. *Polym Test*. 2016;56:261-268. doi:10.1016/j.polymertesting.2016.10.026

15482634, 0, Downloaded from https://4spepublications.onlinelibrary.wiley.com/doi/10.1002/pen.27210 by Ecole De Technologie Superieur, Wiley Online Library on [23/04/2025]. See the Terms and Conditions (https://onlinelibrary.wiley.com/terms-and-conditions) on Wiley Online Library for rules of use; OA articles are governed by the applicable Creative Commons License

26. Kömmling A, Jaunich M, Pourmand P, Wolff D, Hedenqvist M. Analysis of O-ring seal failure under static conditions and determination of end-of-lifetime criterion. *Polymers*. 2019;11:11. doi:10.3390/polym11081251
27. Zaghdoudi M, Kömmling A, Jaunich M, Wolff D. Erroneous or Arrhenius: a degradation rate-based model for EPDM during homogeneous ageing. *Polymers*. 2020;12:12. doi:10.3390/polym12092152
28. Kömmling A, Jaunich M, Wolff D. Effects of heterogeneous aging in compressed HNBR and EPDM O-ring seals. *Polym Degrad Stab*. 2016;126:39-46. doi:10.1016/j.polymdegradstab.2016.01.012
29. Gillen KT, Assink R, Bernstein R, Celina M. Condition monitoring methods applied to degradation of chlorosulfonated polyethylene cable jacketing materials. *Polym Degrad Stab*. 2006;91(6):1273-1288. doi:10.1016/j.polymdegradstab.2005.09.002
30. Gillen KT, Bernstein R. *Review of Nuclear Power Plant Safety Cable Aging Studies with Recommendations for Improved Approaches and for Future Work*. Sandia Report; 2010.
31. Gillen KT, Celina M, Bernstein R. Review of some important issues and resolutions when lifetime predictions of elastomers are made using accelerated aging techniques. presented at: Fall 186th Technical Meeting of Rubber Division, ACS; October 14–16, 2014; Nashville, TN.
32. Harris DJ, Assink RA, Celina M. NMR analysis of oxidatively aged HTPB/IPDI polyurethane rubber: degradation products, dynamics, and heterogeneity. *Macromolecules*. 2001;34:6695-6700. doi:10.1021/ma0108766
33. Celina M, Minier L, Assink R. Development and application of tools to characterize the oxidative degradation of AP/HTPB/Al propellants in a propellant reliability study. *Thermochim Acta*. 2002;384:343-349.
34. Assink RA, Lang DP, Celina M. Condition monitoring of a thermally aged hydroxy-terminated polybutadiene (HTPB)/isophorone diisocyanate (IPDI) elastomer by nuclear magnetic resonance cross-polarization recovery times. *J Appl Polym Sci*. 2001;81(2):453-459. doi:10.1002/app.1457
35. Celina M, Trujillo AB, Gillen KT, Minier LM. Chemiluminescence as a condition monitoring method for thermal aging and lifetime prediction of an HTPB elastomer. *Polym Degrad Stab*. 2006;91(10):2365-2374. doi:10.1016/j.polymdegradstab.2006.04.004
36. Celina M, Skutnik Elliott JM, Winters ST, Assink RA, Minier LM. Correlation of antioxidant depletion and mechanical performance during thermal degradation of an HTPB elastomer. *Polym Degrad Stab*. 2006;91(8):1870-1879. doi:10.1016/j.polymdegradstab.2005.11.006
37. Bensalem K, Eesaee M, Hassanipour M, et al. Lifetime estimation models and degradation mechanisms of elastomeric materials: a critical review. *Polym Degrad Stab*. 2024;220:110644. doi:10.1016/j.polymdegradstab.2023.110644
38. Hamouda I, Eesaee M, Nguyen-Tri P. *Elastomer Service Life: the Role of Thermal and Mechanical Test Data in Predictive Analysis*. Springer Nature Switzerland; 2024:179-205.
39. Marzocca AJ. Evaluation of the polymer–solvent interaction parameter χ for the system cured styrene butadiene rubber and toluene. *Eur Polym J*. 2007;43(6):2682-2689. doi:10.1016/j.eurpolymj.2007.02.034
40. International Organization for Standardization. ISO 11346 Rubber, vulcanized or thermoplastic—estimation of life-time and maximum temperature of use. 2014.
41. Xie J-C, Huang X, Zhang Z-X, Jin G-L, Zhang J-Q, Zhang Y-B. Correlating the time-dependent behavior of EPDM gaskets with the long-term sealant performance of gasketed joints in shield tunnels. *Construct Build Mater*. 2024;419:135526. doi:10.1016/j.conbuildmat.2024.135526
42. Li C, Ding Y, Yang Z, Yuan Z, Ye L. Compressive stress-thermo oxidative ageing behaviour and mechanism of EPDM rubber gaskets for sealing resilience assessment. *Polymer Test*. 2020;84:106366. doi:10.1016/j.polymertesting.2020.106366
43. Zhi J, Wang Q, Zhang M, Zhou Z, Liu A, Jia Y. Coupled analysis on hyper-viscoelastic mechanical behavior and macromolecular network alteration of rubber during thermo-oxidative aging process. *Polymer*. 2019;171:15-24. doi:10.1016/j.polymer.2019.03.029
44. Kashi S, Varley R, Souza MD, et al. Mechanical, thermal, and morphological behavior of silicone rubber during accelerated aging. *Polym-Plast Technol Eng*. 2018;57(16):1687-1696. doi:10.1080/03602559.2017.1419487
45. Bouaziz R, Truffault L, Borisov R, et al. Elastic properties of polychloroprene rubbers in tension and compression during ageing. *Polymers*. 2020;12:2354. doi:10.3390/polym12102354
46. Kadri R, Nait Abdelaziz M, Fayolle B, Ayoub G, Hassine MB, Nziakou Y. Micromechanical based model for predicting aged rubber fracture properties. *Int J Fract*. 2023;243(2):125-142. doi:10.1007/s10704-023-00730-x
47. Hassani F, Faisal NH, Nish R, Rothnie S, Njuguna J. The impact of thermal ageing on sealing performance of HNBR packing elements in downhole installations in oilfield wellhead applications. *J Petrol Sci Eng*. 2022;208:109200. doi:10.1016/j.petrol.2021.109200
48. Balasooriya W, Schrittesser B, Karunakaran S, et al. Influence of thermo-oxidative ageing of HNBR in oil field applications. *Macromol Symp*. 2017;373:373. doi:10.1002/masy.201600093
49. Tu J, Shi X, Jing Y, et al. Relationships of tensile strength with crosslink density for the high-carbon black-filled EPDM compounds with various softeners. *Polym Eng Sci*. 2021;61(8):2213-2221. doi:10.1002/pen.25750
50. Li B, Li S, Shen M, et al. Tribological behaviour of acrylonitrile–butadiene rubber under thermal oxidation ageing. *Polymer Test*. 2021;93:106954. doi:10.1016/j.polymertesting.2020.106954
51. Lee P-C, Kim SY, Ko YK, et al. Durability and service life prediction of fluorocarbon elastomer under thermal environments. *Polymers*. 2022;14:2047. doi:10.3390/polym14102047
52. Redon A, Le Cam JB, Robin E, Miroir M, Fralin JC. Aging characterization of different nitrile butadiene rubbers for sealing in a pneumatic system: linking the change of the physicochemical state to the mechanical properties. *J Appl Polym Sci*. 2023;140(29):e54068. doi:10.1002/app.54068
53. Jiang M, Qin L, Han J, Li Q. Changes in crosslinking structure of thermo-oxidative aging chloroprene rubber and its effect on strain-induced crystallization. *J Appl Polym Sci*. 2024;141(4):e54858. doi:10.1002/app.54858
54. Jovanović S, Samaržija-Jovanović S, Marković G, Jovanović V, Adamović T, Marinović-Cincović M. Mechanical properties and thermal aging behaviour of polyisoprene/polybutadiene/styrene–butadiene rubber ternary blend reinforced with carbon black. *Compos Part B Eng*. 2016;98:126-133. doi:10.1016/j.compositesb.2016.04.060
55. Celina MC. Review of polymer oxidation and its relationship with materials performance and lifetime prediction. *Polym Degrad Stab*. 2013;98:2419-2429. doi:10.1016/j.polymdegradstab.2013.06.024

15482634, 0, Downloaded from https://4spepublications.onlinelibrary.wiley.com/doi/10.1002/pen.27210 by Ecole De Technologie Superieur, Wiley Online Library on [23/04/2025]. See the Terms and Conditions (https://onlinelibrary.wiley.com/terms-and-conditions) on Wiley Online Library for rules of use; OA articles are governed by the applicable Creative Commons License

56. Celina M, Bernstein R, Gillen KT. Challenges of accelerated aging techniques for elastomer lifetime predictions. *Rubber Chem Technol*. 2015;88(1):1-27. doi:10.5254/rct.14.85930
57. Xiang K, Huang G, Zheng J, Wang X, Li GX, Huang J. Accelerated thermal ageing studies of polydimethylsiloxane (PDMS) rubber. *J Polym Res*. 2012;19(5):1-7. doi:10.1007/s10965-012-9869-6
58. Ahagon A, Kida M, Kaidou H. Aging of tire parts during service. I. Types of aging in heavy-duty tires. *Rubber Chem Technol*. 1990;63:683-697. doi:10.5254/1.3538282
59. Baldwin JM, Bauer DR, Ellwood KR. Accelerated aging of tires, part III. *Rubber Chem Technol*. 2005;78(5):767-776. doi:10.5254/1.3547912
60. Ngolemasango EF, Bennett M, Clarke J. Kinetics of the effect of ageing on tensile properties of a natural rubber compound. *J Appl Polym Sci*. 2006;102(11):3732-3740. doi:10.1002/app.24634
61. Baldwin JM, Bauer DR, Ellwood KR. Accelerated aging of tires, part II. *Rubber Chem Technol*. 2005;78(2):336-353. doi:10.5254/1.3547887

How to cite this article: Tayefi M, Eesaee M, Hassanipour M, Elkoun S, David E, Nguyen-Tri P. Thermal aging behavior and lifetime prediction of industrial elastomeric compounds based on styrene–butadiene rubber. *Polym Eng Sci*. 2025; 1-21. doi:10.1002/pen.27210

15482634, 0, Downloaded from https://4spepublications.onlinelibrary.wiley.com/doi/10.1002/pen.27210 by Ecole De Technologie Superieur, Wiley Online Library on [23/04/2025]. See the Terms and Conditions (https://onlinelibrary.wiley.com/terms-and-conditions) on Wiley Online Library for rules of use; OA articles are governed by the applicable Creative Commons License